

Transverse momentum distribution with radial flow in relativistic diffusion model

N. Suzuki^{1a} and M. Biyajima^{2b}

¹ Department of Comprehensive Management, Matsumoto University, Matsumoto 390-1295, Japan

² Department of Physics, Shinshu University, Matsumoto, 390-8621, Japan

Received: date / Revised version: date

Abstract. Large transverse momentum distributions of identified particles observed at RHIC are analyzed by a relativistic stochastic model in the three dimensional (non-Euclidean) rapidity space. A distribution function obtained from the model is Gaussian-like in radial rapidity. It can well describe observed transverse momentum p_T distributions. Estimation of radial flow is made from the analysis of p_T distributions for \bar{p} in Au + Au Collisions. Temperatures are estimated from observed large p_T distributions under the assumption that the distribution function approaches to the Maxwell-Boltzmann distribution in the lower momentum limit. Power-law behavior of large p_T distribution is also derived from the model.

PACS. 25.75.-q Relativistic heavy ion collisions – 13.85.Ni Inclusive production with identified hadrons – 20.50.Ey Stochastic models

1 Introduction

At RHIC colliding energy of nuclei becomes up to 200 AGeV, and thousands of particles are produced per event. To describe such many particle system, a sort of collective approach will be useful. One-particle rapidity or pseudo-rapidity distributions observed at RHIC are well described by the Ornstein-Uhlenbeck process [1, 2].

In order to treat transverse momentum p_T distributions, we can extend one dimensional stochastic equation to a three-dimensional one using variables, longitudinal rapidity and two transverse momenta. The fundamental solution is Gaussian in these variables. Even if the formula is integrated over the azimuthal angle in the transverse momentum plane, the distribution is only slightly modified from the Gaussian in the low p_T region. However, the observed p_T distributions at RHIC have long tails compared with an exponential distribution, and cannot be described by the formula. Therefore relativistic treatment for the transverse direction would be needed as long as the stochastic approach is adopted.

In reference [3], an empirical formula for large p_T distributions at polar angle $\theta = \pi/2$,

$$E \frac{d^3\sigma}{d^3p} \Big|_{\theta=\pi/2} = A \exp \left[-\frac{y_T^2}{2L_T} \right],$$

$$y_T = \frac{1}{2} \ln \frac{E + |\mathbf{p}_T|}{E - |\mathbf{p}_T|}, \quad (1)$$

was proposed from the analogy of Landau's hydrodynamical model. Polar angle θ ($0 \leq \theta \leq \pi$) is measured from the beam direction of colliding nuclei or incident particles. In equation (1), E denotes energy of an observed particle, L_T is a parameter, and y_T is called the "transverse rapidity". Equation (1) well describes large p_T distributions for $p + p \rightarrow \pi^0 + X$ and $p + p \rightarrow \pi^\pm + X$. Recently, large p_T distributions for π^0 in pp collisions observed at RHIC are also analyzed by (1) [4]. However, it cannot be derived from the hydrodynamical model.

The transverse rapidity is defined in the geodesic cylindrical coordinate system in the three dimensional rapidity space, where longitudinal rapidity y , transverse rapidity ξ and azimuthal angle ϕ are used. The longitudinal rapidity y , and the transverse rapidity ξ are defined respectively as,

$$y = \ln \frac{E + p_L}{m_T}, \quad \xi = \ln \frac{m_T + |\mathbf{p}_T|}{m},$$

where E, p_L, \mathbf{p}_T and m denote energy, longitudinal momentum, transverse momentum, and mass of the observed particle, respectively, and $m_T = \sqrt{\mathbf{p}_T^2 + m^2}$. It should be noted that y_T coincides with ξ , only if $\theta = \pi/2$, namely $p_L = 0$.

As for the relativistic approach to stochastic equation, we consider the diffusion equation in the three dimensional rapidity space or Lobachevsky space, which is non-Euclidean. In order to classify the longitudinal and transverse expansion, it would be appropriate to consider the

^a e-mail: suzuki@matsu.ac.jp

^b e-mail: biyajima@azusa.shinshu-u.ac.jp

diffusion equation in the geodesic cylindrical coordinate,

$$\frac{\partial f}{\partial t} = \frac{D}{\cosh^2 \xi} \frac{\partial^2 f}{\partial y^2} + \frac{D}{\sinh \xi \cosh \xi} \frac{\partial}{\partial \xi} \left(\sinh \xi \cosh \xi \frac{\partial f}{\partial \xi} \right) + \frac{D}{\sinh^2 \xi} \frac{\partial^2 f}{\partial \phi^2}, \quad (2)$$

where D denotes a diffusion constant. However, we cannot solve (2) at present, as far as we are aware. Therefore, we should consider somewhat simpler case.

We have proposed the relativistic diffusion model where an effect of radial flow is not included, and analyzed large p_T distributions for charged particles [5] and identified particles [6] in $Au+Au$ collisions. The distribution function of it is Gaussian-like in radial rapidity ρ , which coincides with ξ at $\theta = \pi/2$, and resembles with (1) at $\theta = \pi/2$.

In section 2, the relativistic diffusion model, where the flow effect is taken into account, is briefly explained. In section 3, large p_T distributions in $p+p \rightarrow \pi^0 + X$ and in $Au+Au \rightarrow \pi^0 + X$ at $\sqrt{s_{NN}} = 200$ GeV observed at RHIC [7,8,9] are analyzed. In section 4, a flow effect or a transverse flow velocity is estimated from p_T distributions in $Au+Au \rightarrow \bar{p} + X$, and p_T distributions for π^0 , π^- and K^- are analyzed by the use of the transverse flow velocity estimated from p_T distributions of \bar{p} . A possible interpretation of the dispersion of the Gaussian-like distribution is shown in section 5. The higher transverse momentum limit of our model is discussed in section 6. Final section is devoted to summary and discussions.

2 Diffusion equation in the three dimensional rapidity space

For simplicity, we consider the diffusion equation with radial symmetry in the three dimensional geodesic polar coordinate system,

$$\frac{\partial f}{\partial t} = \frac{D}{\sinh^2 \rho} \frac{\partial}{\partial \rho} \left(\sinh^2 \rho \frac{\partial f}{\partial \rho} \right), \quad (3)$$

with an initial condition,

$$f(\rho, t=0) = \frac{\delta(\rho - \rho_0)}{4\pi \sinh^2 \rho}. \quad (4)$$

In equation (3), ρ denotes the radial rapidity, which is written with energy E , momentum \mathbf{p} and mass m of observed particle,

$$\rho = \ln \frac{E + |\mathbf{p}|}{m}. \quad (5)$$

Inversely, energy and momentum are written respectively as

$$E = m \cosh \rho, \quad |\mathbf{p}| = \sqrt{p_L^2 + \mathbf{p}_T^2} = m \sinh \rho. \quad (6)$$

The solution [10] of (3) with the initial condition (4) is given by

$$f(\rho, \rho_0, t) = \frac{1}{2\pi \sqrt{4\pi Dt}} e^{-Dt} \times \frac{\sinh \frac{\rho_0 \rho}{2\pi Dt}}{\sinh \rho_0 \sinh \rho} \exp \left[-\frac{\rho^2 + \rho_0^2}{4Dt} \right]. \quad (7)$$

A physical picture described by (3) and (4) is as follows; After a collision of nuclei, particles are produced at radial rapidity ρ_0 expressed by (4). Then those particles propagate according to the diffusion equation (3). In the course of the space time development, energy is supplied from the leading particle system (collided nuclei) to the produced particle system. Number density of particles becomes lower and at some (critical) density, interactions among secondary particles cease, and particles become free.

From equation (7), the following equation [11] is obtained;

$$f(\rho, t) = \lim_{\rho_0 \rightarrow 0} f(\rho, \rho_0, t) = (4\pi Dt)^{-3/2} e^{-Dt} \frac{\rho}{\sinh \rho} \exp \left[-\frac{\rho^2}{4Dt} \right]. \quad (8)$$

Transverse momentum (rapidity) distributions at fixed polar angle θ are analyzed by (7) or (8), where transverse momentum is given by $|\mathbf{p}_T| = m \sinh \rho \sin \theta$.

In order to clarify our approach to the previous non-relativistic approach [12,13], equation (7) is compared with the solution for the radial symmetric diffusion equation in the Euclidean space in appendix A.

3 Analysis of p_T distributions observed at RHIC

At first, transverse momentum (rapidity) distributions of identified particles observed by the PHENIX collaboration [7,8,9] are analyzed by the use of (8),

$$f(\rho, t) = C (2\pi \sigma(t)^2)^{-3/2} e^{-\sigma(t)^2/2} \times \frac{\rho}{\sinh \rho} \exp \left[-\frac{\rho^2}{2\sigma(t)^2} \right], \quad \sigma(t)^2 = 2Dt, \quad (9)$$

with parameters, C and $\sigma(t)^2$ ¹.

As the data are taken at $\theta = \pi/2$ or $p_L = 0$, the identity $\rho = \xi = y_T$ is satisfied. In the analysis, we use $m_{\pi^0} = 135$, $m_{\pi^-} = 140$, $m_{K^-} = 494$, and $m_{\bar{p}} = 938$ MeV.

The result on the p_T distribution in $p+p \rightarrow \pi^0 + X$ is shown in Fig. 1. Solid curve in Fig. 1 is drawn by the use of (9), parameters of which are estimated with the least square method, and are shown in Table 1. Observed p_T

¹ Somewhat different analyses based on statistical models and the different stochastic model have been made in [14]

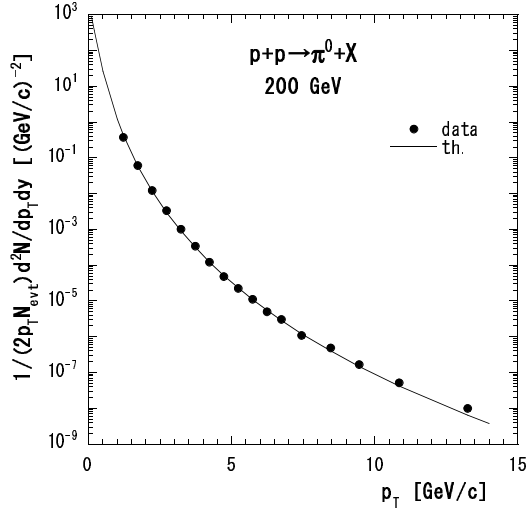


Fig. 1. p_T distribution for $p + p \rightarrow \pi^0 + X$ at $y = 0$ [7]

Table 1. Parameters on p_T distributions estimated by (9) in $p + p \rightarrow \pi^0 + X$ at $y = 0$ at $\sqrt{s} = 200$ GeV [7]

C	$\sigma(t)^2$	$\chi^2/\text{n.d.f.}$
13547.3 ± 941.7	0.603 ± 0.004	12.3/15

Table 2. Parameters on p_T distributions estimated by (9) in $Au + Au \rightarrow \pi^0 + X$ at $y = 0$ at $\sqrt{s_{NN}} = 200$ GeV [8]

centrality	C	$\sigma(t)^2$	$\chi^2/\text{n.d.f.}$
min.bias	45066.0 ± 4542.7	0.586 ± 0.004	28.0/22
00-10%	146819.0 ± 16095.3	0.574 ± 0.005	27.3/16
10-20%	103772.0 ± 11348.3	0.580 ± 0.005	20.0/15
20-30%	69568.0 ± 7647.8	0.586 ± 0.005	14.9/13
30-40%	43168.0 ± 4870.7	0.592 ± 0.006	15.7/13
40-50%	25292.0 ± 2955.2	0.600 ± 0.006	9.4/12
50-60%	13800.3 ± 1629.2	0.600 ± 0.007	12.4/12
60-70%	5477.2 ± 699.8	0.617 ± 0.008	8.2/10
70-80%	2498.80 ± 336.74	0.616 ± 0.009	7.2/9
80-92%	1275.89 ± 216.03	0.610 ± 0.011	5.0/8

distributions for π^0 in $p + p$ collisions are well described by (9) from 1.2 GeV/c to 13.2 GeV/c.

The results on p_T distributions in $Au + Au \rightarrow \pi^0 + X$ are shown in Fig. 2 and Table 2. As can be seen from Fig. 2 and Table 2, observed p_T distributions on π^0 in $Au + Au$ collisions are well described by (9) from centrality 0-10% to centrality 80-92 %.

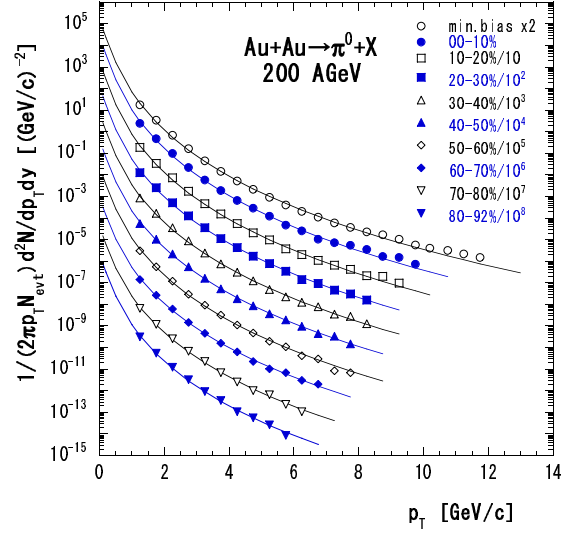


Fig. 2. p_T distribution for $Au + Au \rightarrow \pi^0 + X$ at $y = 0$ [8]

4 Estimation of radial flow

We have analyzed large p_T distributions in $Au + Au \rightarrow \pi^0 + X$ in the previous section. However, if the effect of flow in the transverse direction is taken into account, estimated values of parameters would be different from those shown in Table 2.

The effect of transverse flow in $Au + Au$ collisions at $\sqrt{s_{NN}} = 200$ GeV is estimated from the observed p_T distribution in $Au + Au \rightarrow \bar{p} + X$ from $p_T = 0.65$ GeV/c to $p_T = 4.25$ GeV/c by the use of the formula,

$$f(\rho, \rho_0, t) = \frac{C}{2\pi\sqrt{2\pi\sigma(t)^2}} e^{-\sigma(t)^2/2} \times \frac{\sinh \frac{\rho_0 \rho}{\sigma^2(t)}}{\sinh \rho_0 \sinh \rho} \exp \left[-\frac{\rho^2 + \rho_0^2}{2\sigma(t)^2} \right]. \quad (10)$$

The results are shown in Fig. 3 and Table 3. From Table 3, we can obtain the transverse flow velocity v_0 using the relation $v_0 = \tanh \rho_0$. It varies from $v_0 = \tanh 0.82 = 0.68$ at centrality 00-05% to $v_0 = 0.42$ at centrality 80-92% ($v_0 = 0.39$ at centrality 70-80%). As the relation of centrality to the average number of participant nucleons $\langle N_{prt} \rangle$ is given in Refs. [7] and [8], we can fit the estimated values of ρ_0 as a function of $\langle N_{prt} \rangle$;

$$\rho_0 = 0.113 \ln(x) + 0.164, \quad x = \langle N_{prt} \rangle. \quad (11)$$

The result is shown in Fig. 4.

Then, we analyze observed p_T distributions with ρ_0 given by (11), and $\langle N_{prt} \rangle$, which is shown in [8]. The results on π^0 , π^- and K^- are shown respectively in Tables 4, 5 and 6.

Table 3. Parameters on p_T distributions estimated by (10) in $Au + Au \rightarrow \bar{p} + X$ at $y = 0$ at $\sqrt{s_{NN}} = 200$ GeV [9]

centrality	C	$\sigma(t)^2$	ρ_0	$\chi^2/\text{n.d.f}$
00-05%	17.713 ± 0.626	0.138 ± 0.008	0.820 ± 0.029	4.5/19
05-10%	14.974 ± 0.538	0.141 ± 0.009	0.803 ± 0.030	5.4/19
10-15%	12.508 ± 0.454	0.144 ± 0.009	0.795 ± 0.032	4.4/19
15-20%	10.492 ± 0.389	0.147 ± 0.010	0.778 ± 0.034	3.7/19
20-30%	7.762 ± 0.293	0.148 ± 0.009	0.759 ± 0.034	3.2/19
30-40%	5.175 ± 0.209	0.158 ± 0.011	0.705 ± 0.041	1.0/10
40-50%	3.168 ± 0.137	0.167 ± 0.001	0.647 ± 0.051	2.3/19
50-60%	1.8169 ± 0.0877	0.172 ± 0.001	0.587 ± 0.066	1.8/19
60-70%	0.8949 ± 0.0489	0.191 ± 0.001	0.459 ± 0.127	1.0/19
70-80%	0.3638 ± 0.0239	0.190 ± 0.001	0.409 ± 0.211	6.1/19
80-92%	0.1821 ± 0.0157	0.167 ± 0.001	0.444 ± 0.195	2.6/17

Table 4. Parameters on p_T distributions estimated by (10) with (11) in $Au + Au \rightarrow \pi^0 + X$ at $y = 0$ at $\sqrt{s_{NN}} = 200$ GeV [8]

centrality	C	$\sigma(t)^2$	ρ_0	$\chi^2/\text{n.d.f}$
min.bias	27977.0 ± 2764.2	0.500 ± 0.004	0.694	29.8/22
00-10%	72773.0 ± 7625.2	0.469 ± 0.005	0.818	24.2/16
10-20%	56883.0 ± 5936.0	0.479 ± 0.005	0.781	17.0/15
20-30%	41647.0 ± 4386.1	0.490 ± 0.005	0.742	10.3/13
30-40%	27513.0 ± 3012.5	0.503 ± 0.005	0.699	13.1/13
40-50%	17515.0 ± 2002.8	0.518 ± 0.006	0.651	7.6/12
50-60%	10559.0 ± 1224.0	0.526 ± 0.006	0.595	9.2/12
60-70%	4548.40 ± 578.86	0.553 ± 0.008	0.531	7.2/10
70-80%	2241.30 ± 313.24	0.564 ± 0.009	0.457	6.4/9
80-92%	1178.50 ± 204.72	0.574 ± 0.011	0.372	4.9/8

Table 5. Parameters on p_T distributions estimated by (10) with (11) in $Au + Au \rightarrow \pi^- + X$ at $y = 0$ at $\sqrt{s_{NN}} = 200$ GeV [9]

centrality	C	$\sigma(t)^2$	ρ_0	$\chi^2/\text{n.d.f}$
00-05%	32150.0 ± 846.3	0.533 ± 0.003	0.826	357.4/26
05-10%	27161.0 ± 718.2	0.546 ± 0.003	0.808	308.0/26
10-15%	22407.0 ± 594.1	0.559 ± 0.004	0.790	271.1/26
15-20%	18795.0 ± 501.4	0.566 ± 0.004	0.781	217.5/26
20-30%	14332.0 ± 383.4	0.582 ± 0.004	0.742	195.3/26
30-40%	9337.0 ± 254.4	0.603 ± 0.004	0.699	136.9/26
40-50%	5773.6 ± 161.0	0.617 ± 0.004	0.651	108.6/26
50-60%	3365.10 ± 96.36	0.629 ± 0.005	0.595	91.0/26
60-70%	1729.70 ± 51.22	0.640 ± 0.005	0.531	80.8/26
70-80%	784.01 ± 24.37	0.655 ± 0.006	0.457	54.4/26
80-92%	393.59 ± 12.88	0.664 ± 0.007	0.372	39.9/26

As can be seen from Tables 4 and 5, fitting of our calculation by (10) to the data is better than that by (9) except for the minimum bias events in $Au + Au \rightarrow \pi^0 + X$. The fit to π^- distributions is not so good as that to π^0 distributions. The result at lower centrality is no good, but it is much improved as the centrality increases.

5 Possible interpretation of parameter $\sigma(t)^2$

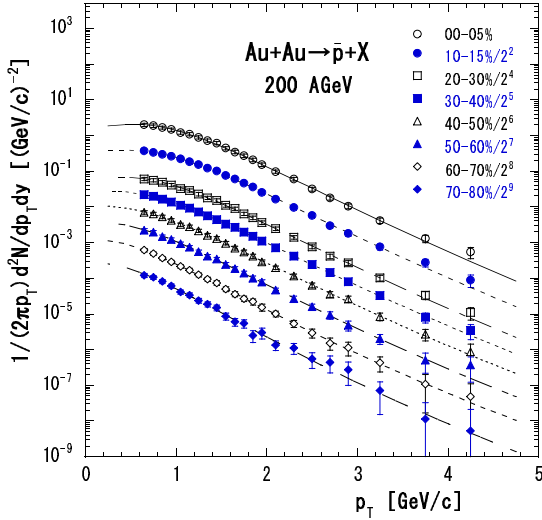
In order to get a possible interpretation of parameter $\sigma(t)^2$, an approximate expression of (9) in the small $|\mathbf{p}_T|$ region is taken. When $\rho < 1$, $|\mathbf{p}| = m \sinh \rho \simeq m\rho$. Then, (9) reduces to

The results by (10) on π^- and K^- are also better than those by (9), which are not shown for brevity.

$$f(\rho, t) \simeq \exp \left[-\frac{\rho^2}{2\sigma(t)^2} \right]. \quad (12)$$

Table 6. Parameters on p_T distributions estimated by (10) with (11) in $Au + Au \rightarrow K^- + X$ at $y = 0$ at $\sqrt{s_{NN}} = 200$ GeV [9]

centrality	C	$\sigma(t)^2$	ρ_0	$\chi^2/\text{n.d.f}$
00-05%	254.63 ± 8.93	0.258 ± 0.008	0.826	0.52/14
05-10%	212.58 ± 7.45	0.266 ± 0.008	0.808	0.62/14
10-15%	175.59 ± 6.20	0.269 ± 0.008	0.790	0.87/14
15-20%	145.12 ± 5.17	0.271 ± 0.008	0.781	0.92/14
20-30%	108.69 ± 3.89	0.286 ± 0.008	0.742	1.07/14
30-40%	70.370 ± 2.579	0.290 ± 0.008	0.699	1.70/14
40-50%	42.070 ± 1.577	0.302 ± 0.008	0.651	1.80/14
50-60%	23.404 ± 0.918	0.311 ± 0.009	0.595	2.76/14
60-70%	11.308 ± 0.465	0.320 ± 0.009	0.531	3.51/14
70-80%	4.782 ± 0.215	0.329 ± 0.011	0.457	3.75/14
80-92%	2.274 ± 0.113	0.342 ± 0.013	0.372	7.59/14

**Fig. 3.** p_T distribution for $Au + Au \rightarrow \bar{p} + X$ at $y = 0$ [8], analyzed by (10), where ρ_0 is included.

If we assume that equation (12) should coincide with the Maxwell-Boltzmann distribution,

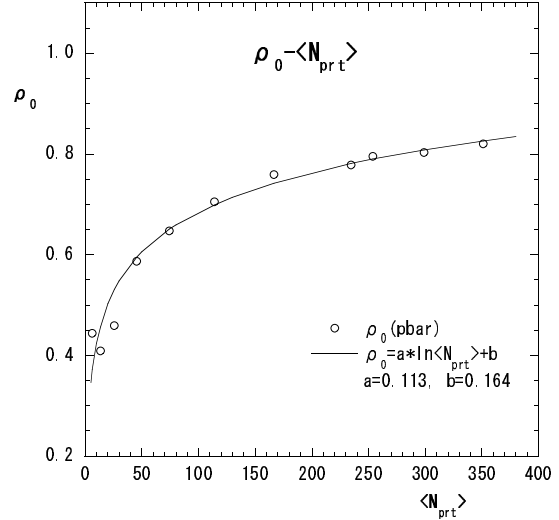
$$f(\mathbf{v}) = \left(\frac{m}{2\pi k_B T} \right)^{3/2} \exp \left[-\frac{m\mathbf{v}^2}{2k_B T} \right],$$

where k_B is the Boltzmann constant, then we have an identity,

$$k_B T = m\sigma(t)^2. \quad (13)$$

Equation (13) is obtained in the lower momentum limit, namely, with the condition that $\rho \ll 1$.

From (13), we can estimate the temperature $k_B T$ of inclusive reactions for observed particle with mass m . The results are shown in Fig. 5. The estimated temperature

**Fig. 4.** Dependence of ρ_0 to average number of participants in $Au + Au$ collisions estimated by (11)

$k_B T$ from the p_T distributions for π^0 is from 63.3 MeV at centrality 5-10% to 77.5 MeV at centrality from 80-92%, and that for π^- is from 74.8 MeV at centrality 0-5% to 93.1 MeV at centrality from 80-92%. The temperature of π^0 or π^- , estimated from (13), is somewhat lower than that from the exponential function of p_T . This would be affected by the assumption $\rho \ll 1$ used to obtain the identity (13).

The estimated temperature from the p_T distributions for K^- is from 128.0 MeV at centrality 0-5% to 163.5 MeV at centrality from 80-92%. That for \bar{p} distributions is from 128.5 MeV at centrality 0-5% to 172.6 MeV at centrality from 80-92%. The results on \bar{p} distributions shown in Fig. 5 are recalculated by the use of (12).

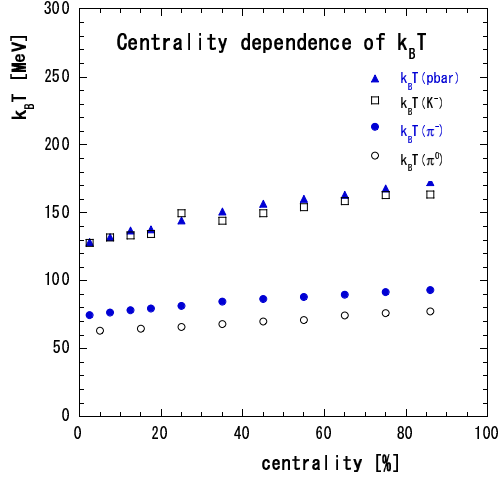


Fig. 5. Centrality dependence of temperature $k_B T$ estimated by (10) with (11) from p_T distributions in $Au + Au$ collisions

6 Higher transverse momentum limit of the model

In the 1970's, when large p_T distributions are observed in accelerator experiments, many models, which have power-law behavior in p_T are proposed [15]. In [16], a model for p_T distribution, inspired by QCD, is proposed as $(p_0/(p_T + p_0))^n$. In the following, $|\mathbf{p}_T|$ is abbreviated to p_T . It approaches an exponential distribution of p_T for $p_T \rightarrow 0$, and a power function of p_T for $p_T \rightarrow \infty$.

In this section, it is derived that equation (7) at $\theta = \pi/2$ shows power-law behavior in p_T in the higher p_T limit, when the identity $\rho = \ln((m_T + p_T)/m)$ is used.

The following two terms in (7) can be rewritten in the power form of $m_T + p_T$ as;

$$\begin{aligned} \sinh \frac{\rho_0 \rho}{\sigma^2(t)} &= \frac{1 - e^{-2\rho_0 \rho / \sigma^2(t)}}{2} e^{\rho_0 \rho / \sigma^2(t)} \\ &\simeq \frac{1}{2} \left(\frac{m_T + p_T}{m} \right)^{\rho_0 / \sigma(t)^2}, \\ \sinh \rho &= \frac{1 - e^{-2\rho}}{2} e^\rho \simeq \frac{1}{2} \left(\frac{m_T + p_T}{m} \right). \end{aligned}$$

Radial rapidity contained in the Gaussian-like part in (10) is rewritten as,

$$\exp \left[-\frac{\rho^2}{2\sigma(t)^2} \right] = \left(\frac{m_T + p_T}{m} \right)^{-\rho/2\sigma(t)^2}. \quad (14)$$

As is well known that a logarithmic distribution of x has weaker dependence compared with a power-law distribution of x with any positive exponent in the limit of $x \rightarrow \infty$, we have,

$$\lim_{p_T \rightarrow \infty} \frac{\rho}{p_T^\epsilon} = \lim_{p_T \rightarrow \infty} \frac{1}{p_T^\epsilon} \ln \left(\frac{m_T + p_T}{m} \right) = 0$$

for any positive number ϵ . Therefore, we can approximate ρ in the exponent in (14) as constant, which is written by $2c_0$, within some finite transverse momentum range. Then (10) is reduced to the form,

$$\begin{aligned} f(\rho, \rho_0, t) &\sim \left(\frac{m}{m_T + p_T} \right)^{(c_0 - \rho_0)/\sigma(t)^2 + 1} \\ &\sim \left(\frac{m}{2p_T} \right)^{(c_0 - \rho_0)/\sigma(t)^2 + 1}. \end{aligned} \quad (15)$$

From equation (15), one can see that equation (10) shows power-law behavior in the higher transverse momentum limit, and that the power becomes smaller as ρ_0 increases, and it also becomes smaller as $\sigma(t)^2$, which should increase with the colliding energy $\sqrt{s_{NN}}$, increases.

7 Summary and discussions

In order to analyze large p_T distributions of charged particles observed at RHIC, the relativistic stochastic process in the three dimensional rapidity space, which is non-Euclidean, is introduced. The solution is Gaussian-like in radial rapidity, where the radial flow rapidity ρ_0 is included. It is very similar to the formula proposed in [3] at $\theta = \pi/2$.

Transverse momentum distributions for π^0 in pp collisions at $y = 0$ at $\sqrt{s} = 200$ GeV observed by the PHENIX collaboration are analyzed. Observed p_T distributions are well described by the formula (9) from 1.2 GeV/c to 13.2 GeV/c

In $Au + Au$ collisions, firstly, we analyzed the data for π^0 using (9), where flow effect is not included, i.e. $\rho_0 = 0$. The formula (9) well describes the observed p_T distributions.

Next, we have analyzed the observed p_T distributions for $Au + Au \rightarrow \bar{p} + X$ using (10). In the formula, non-zero radial rapidity ρ_0 at the initial stage, which corresponds to the radial flow velocity $v_0 = \tanh \rho_0$, is included.

The temperature is estimated under the assumption that (4) approaches to the Maxwell-Boltzmann distribution when $\rho \ll 1$ or $p_T \ll m$.

In our analysis, non-zero value of the radial flow rapidity (or radial flow velocity) has an influence on the estimation of temperature. One can see the effect of ρ_0 from (15). In addition, all of the minimum chi-squared values by the use of (10) with (11) become smaller than those with $\rho_0 = 0$ except for the minimum bias events in $Au + Au \rightarrow \pi^0 + X$.

We have derived that our formula (10) shows power-law behavior in p_T in the higher transverse momentum limit. Therefore, it behaves like a Gaussian distribution in p_T when $p_T \ll m$, and like a power-law distribution in p_T when $p_T \gg 1$.

Acknowledgement

Authors would like to thank RCNP at Osaka University, Faculty of Science, Shinshu University, and Matsumoto University for financial support.

A Relation to non-relativistic approach

The radial symmetric diffusion equation in the n ($n = 2, 3$) dimensional Euclidean space is written as,

$$\frac{\partial f}{\partial t} = D \frac{\partial^2 f}{\partial r^2} + \frac{D(n-1)}{r} \frac{\partial f}{\partial r}. \quad (16)$$

The solution of (16) with the initial condition

$$f(r, t=0) = \frac{\delta(r-r_0)}{2\pi(2r_0)^{n-1}} \quad (17)$$

is given by [17],

$$f(r, r_0, t) = \frac{1}{2Dt} \exp \left[-\frac{r^2 + r_0^2}{4Dt} \right] \times (r_0 r)^{-(n-2)/2} I_{(n-2)/2} \left(\frac{r_0 r}{2Dt} \right). \quad (18)$$

In the case of two dimensional expansion, $n = 2$, (18) coincides with the formula in [12], if $2Dt = m/T$, $r = |\mathbf{p}_T|/m$, and $r_0 = |\mathbf{p}_{T0}|/m$.

Using the identity

$$\sinh z = \sqrt{\pi z/2} I_{1/2}(z),$$

we can rewrite (7) as

$$f(\rho, \rho_0, t) = \frac{1}{8\pi Dt} e^{-Dt} \frac{(\rho_0 \rho)^{1/2}}{\sinh \rho_0 \sinh \rho} \times \exp \left[-\frac{\rho^2 + \rho_0^2}{4Dt} \right] I_{1/2} \left(\frac{\rho_0 \rho}{2Dt} \right). \quad (19)$$

In the case of the three dimensional expansion in the Euclidean space, comparing (19) with (18) at $n = 3$, one can recognize that (19) is a relativistic extension of (18), and that (19) reduces to (18) in the low momentum region, $|\mathbf{p}| \ll 1$, where $|\mathbf{p}| = m \sinh \rho \simeq m\rho$ and $\sinh \rho_0 \simeq \rho_0$.

References

1. M. Biyajima, M. Ide, T. Mizoguchi and N. Suzuki, Prog. Theor. Phys. **108**, (2002) 559; Addendum **109**, (2003) 151; M. Biyajima, M. Ide, M. Kaneya, T. Mizoguchi and N. Suzuki, Prog. Theor. Phys. Suppl. **153**, (2004) 3449
2. G. Wolschin, Eur. Phys. J. **A5**, (1999) 85; Phys. Rev. **C69**, (2004) 024906
3. M. Duong-van M and P. Carruthers, Phys. Rev. Lett. **31**, (1973) 133
4. Steinberg P, preprint nucl-ex/0405022
5. N. Suzuki and M. Biyajima, Acta Phys. Pol. **B35**, (2004) 283
6. N. Suzuki and M. Biyajima, preprint hep-th/0404112, unpublished
7. S. S. Adler, et al. PHENIX collaboration, Phys. Rev. Lett. **91**, (2003) 072301
8. S. S. Adler, et al. PHENIX collaboration, Phys. Rev. Lett. **91**, (2003) 241803
9. S. S. Adler, et al. PHENIX collaboration, nucl-ex/0307022
10. N. Suzuki and M. Biyajima, math-ph/0406040, unpublished
11. F. I. Karpelevich, V. N. Tutubalin and M. G. Shur, Theory Prob. Applications **4**, (1959) 432; Molchanov S A, Russian Math. Surveys **30**, (1976) 1007
12. Voloshin S, Phys. Rev. **C55**, (1997) 1630
13. Sasaki N, Miyamura O, Muroya S and Nonaka C, 2001 *Europhys. Lett.* **54** 38
14. M. Biyajima, M. Kaneya, T. Mizoguchi and G. Wilk, Eur. Phys. J. **C40**, (2005) 243
15. J. D. Bjorken, Acta Phys. Polon. **B5**, (1974) 893
16. R. Hagedorn, CERN preprint Ref.TH.3684-CERN, 1983
17. W. Feller, Ann. Math. **54**, (1951) 173